Diagnostics of gear faults based on EMD and automatic selection of intrinsic mode functions

Roberto Ricci, Paolo Pennacchi
Department of Mechanical Engineering
Politecnico di Milano
Via La Masa, 1
20156 Milan, Italy
roberto1.ricci@mail.polimi.it, paolo.pennacchi@polimi.it

Abstract

Signal processing is an important tool for diagnostics of mechanical systems. Many different techniques are available to process experimental signals, among others: FFT, wavelet transform, cepstrum, demodulation analysis, second order ciclostationarity analysis, etc. However, often hypothesis about data and computational efforts restrict the application of some techniques. In order to overcome these limitations, the empirical mode decomposition has been proposed. The outputs of this adaptive approach are the intrinsic mode functions that are treated with the Hilbert transform in order to obtain the Hilbert-Huang spectrum.

Anyhow, the selection of the intrinsic mode functions used for the calculation of Hilbert-Huang spectrum is normally done on the basis of user's experience. On the contrary, in the paper a merit index is introduced that allows the automatic selection of the intrinsic mode functions that should be used. The effectiveness of the improvement is proven by the result of the experimental tests presented and performed on a test-rig equipped with a spiral bevel gearbox, whose high contact ratio made difficult to diagnose also serious damages of the gears. This kind of gearbox is normally never employed for benchmarking diagnostics techniques. By using the merit index, the defective gearbox is always univocally identified, also considering transient operating conditions.

Keywords: gearbox diagnostics, empirical mode decomposition, Hilbert transform, Hilbert-Huang spectrum, spiral bevel gear.

1. Introduction

Diagnostics is based on the characterization of mechanical system condition and allows early detection of a possible fault. Whatever the mechanical system, the evaluation of both the type and the fault position allows in a reduction of the plant standstill time. Therefore, from an industrial point of view, a proper diagnostics approach reduces both the time and the costs required for repairing. These considerations have encouraged investments of resources in the diagnostic field.

Signal processing is an approach widely used in diagnostics, since it allows directly characterizing the state of the system. Several types of advanced signal processing techniques have been proposed in the last decades and added to more conventional ones. Since each technique is based on different theoretical background, also the results obtained are often different. Some techniques may be more suitable than others for a specific system or component, depending also on the environmental conditions. Therefore, it is important to choose techniques that are the most effective for the case and the situation under testing for a reliable mechanical analysis.

Gearboxes are components widely used in several industrial fields, like electric power systems, automotive, railways transportation, ships, helicopters, etc. Several signal processing techniques have been proposed for monitoring and diagnostics of spur gear gearboxes in literature. Early papers about this topic are those of McFadden [1, 2, 3], in which the time synchronous average (TSA) signal is introduced. TSA is suitable for both diagnostic purposes and generation of the reference signal for other and more complex signal processing techniques, since it is based on the periodicity and the stationarity of the original signal.

The possibility to analyze the phenomenon in both time and frequency domain has been satisfied by the implementation of time-frequency signal processing techniques. An example is represented by the wavelet transform, which has been applied for spur gear condition monitoring in [4, 5, 6, 7]. The main drawback of this approach is the necessity to know a priori the frequencies of the original signal that should be analyzed. The signal processing in this case is not completely automatic and the computational efforts are proportional to the number of the considered frequencies.

Second order cyclostationary approach is a frequency-frequency analysis. Indeed the spectral correlation density (SCD) is obtained by means of a double transformation in the frequency domain of the auto-correlation of the original signal. Several papers ([8, 9, 10, 11]) are devoted to the application of second order cyclostationary to rotating components: the effectiveness of this technique for bearing and gearbox diagnostics has been proved.

Cepstrum is another signal processing technique, suitable for diagnostics purposes. The cepstrum signal, defined in the quefrency domain, can be obtained by inverse Fourier transform of the auto-spectrum logarithm. The families of rahmonics identifiable in the new domain are directly related to the frequency characterizing the phenomenon ([12, 13]).

The demodulation technique is based on the narrow-band analysis. This methodology is very effective when high amplitude components surrounded by side-bands can be traced in the spectrum. The demodulation analysis has been carried out for spur gearboxes in [14] and improved for spiral bevel gearboxes diagnostics in [15]. All the previously discussed monitoring techniques are compared in [15] and [16].

The signal processing techniques just discussed are usually applied to spur gears. Moreover each of the described methodologies has some drawbacks: almost all provide good results if applied to the TSA signal acquired on the system ([15, 16]), but the synchronous average can be evaluated only if the signal is periodical and stationary. Furthermore some techniques have a reduced degree of automation: in other words, the monitoring and the diagnostic phase require the interaction of a skilled user.

An advanced signal processing methodology suitable for mechanical systems in general and for rotating components like gearboxes in particular, should have the following characteristics:

i) eligible for non-stationary and non-periodic signals: analysis based intrinsically on data (adaptive analysis);
ii) high robustness;
iii) suitable for on-line diagnosis (i.e. fast and not computationally expensive).

The first point of the previous list can be realized by means of a technique allowing the signal to be processed independently from its "shape". The empirical mode decomposition (EMD) and the following Hilbert transform (HT) belong to this kind of methodologies. The milestone of this approach is the paper of Huang et al. [17] in which the algorithm is applied to the experimental signals acquired during natural phenomena (i.e. earthquakes, tsunamis and winds). EMD is useful for the extraction of the intrinsic mode functions (IMFs), or monocomponent functions, composing the original signal, while HT of the extracted functions is used for the instantaneous frequency evaluation. In recent years a number studies used this data-based technique with the aim of applying it to mechanical signals too.

Loutridis applies EMD and HT to spur gearboxes in [18]. In this study, the modelling of the dynamical behaviour of gear meshing with different stage of tooth crack was firstly proposed. Subsequently also experimental signals acquired on a spur transmission were considered.

An improvement of EMD effectiveness is presented by Lei et al. in [19] introducing the enhanced empirical mode decomposition (EEMD), in which the problem of the mixing modes is partially solved by means of the application of white noise to the original signal. This improvement has direct effect on the diagnostic effectiveness of the algorithm, but it is worth to note that the EEMD is more expensive than the EMD from a computational point of view, because many trials are required, due to the additional noise process.

Parey et al. [20] propose an improved model for the simulation of the torsional vibration for a spur gear pair. Both the simulated and the experimental signals are decomposed by means of EMD and statistical parameters are evaluated on the obtained IMFs. It is demonstrated that the kurtosis of IMF allows detecting the fault before the same statistical parameter calculated on the original signal. Other papers, that partially address the EMD scheme, are [21-28].

Since all the existing papers consider spur gearboxes, the diagnostic capability of EMD and HT algorithms for the spiral bevel transmissions is an uncovered field of research. This kind of gearing is an interesting benchmark for

diagnostic techniques, since it has higher contact ratio than spur gears [29]. Thus it is very interesting to verify if a diagnostic technique is able to detect and to discriminate the impending fault in this kind of gearing. Moreover an interesting improvement is presented for the automation of the methodology. The selection of the IMF to be analyzed by means of HT is normally done on the basis of user's experience; instead, in the paper, the authors propose a merit index that automatically selects the IMF to be analyzed. The effectiveness of the proposed method is proven by means of experimental validation. Using the merit index, EMD and HT become an advanced signal processing tool having the characteristics previously listed with a high degree of automation.
The paper is organized as follows: the main steps of the EMD and the HT algorithms are discussed in section 2 and 3 respectively. In section 4 the experimental test-rig is described; the experimental results are shown and discussed in section 5. The conclusions about the effectiveness and the diagnostics capability of the method are reported in section 6.

2. Empirical mode decomposition algorithm

Conversely to other transformations, EMD is an *adaptive decomposition* (i.e. data-based). No hypothesis about signal periodicity or stationarity must be respected for EMD application. The meaning of adaptive decomposition will be clear with the explanation of the EMD algorithm. For the sake of brevity, only the main steps of the procedure will be presented: for a deeper discussion see [17]. The decomposition starts with the research of the maxima and the minima along the signal $x(t)$: all the stationary points are stored. Subsequently all the maxima are interpolated by means of a spline ($s_{\max}(t)$) and the same operation is executed for the minima ($s_{\min}(t)$).
The two splines actually represent the boundaries of the signal $x(t)$: all the points of the signal are in fact included in the space between the two curves. Thanks to the definition of the interpolating splines, the extraction of a mean function $m(t)$ is possible and it can be removed from the initial signal $x(t)$ in order to obtain:

$$x_1(t) = x(t) - m(t) \tag{1}$$

The obtained signal $x_1(t)$ is now examined with the aim to evaluate if it respects the IMF definition. Two main conditions must be satisfied [17, 18]:

- the number of extremes and the number of zero crossing must be equal or only a difference of one is allowed;
- the mean between the local maxima envelope and the local minima envelope at any point (i.e. at any time t) must be equal to zero.

If the two previous conditions are not satisfied, i.e. the resulting signal $x_1(t)$ is not an IMF, then the previous steps are repeated. The procedure becomes iterative and it is called *sifting process*. Obviously functions $s_{\max}(t)$, $s_{\min}(t)$ are recomputed at each iteration and the newly evaluated $m(t)$ is subtracted from the obtained signal $x_1(t)$.
The sifting process runs until the extracted signal respects the two IMF conditions; then the function obtained represents the first intrinsic mode function $C_1(t)$ and it is subtracted from the initial signal:

$$r_1(t) = x(t) - C_1(t) \tag{2}$$

where $r_1(t)$ is the residual signal. This signal represents the input for the second IMF calculation by means of the sifting process. The EMD algorithm, applied to the original signal $x(t)$, stops when the residual signal $r_N(t)$ is a constant or monotonic function, after the extraction of the $N-th$ intrinsic mode function. The stop criteria can be expressed in terms of a standard deviation and number of extremes:

$$\begin{gathered} \sigma\left(r_N(t)\right) < \sigma_{stop}; \\ n_{\max} \text{ and } n_{\min} = 0 \end{gathered} \tag{3}$$

The decomposition stops when both conditions are satisfied.

Since the decomposition objective is the identification of all the original signal structures, the original data can be reconstructed by adding the extracted IMFs to the residual signal.

The effectiveness of the decomposition is evaluated by means of the index of orthogonality (IO) [17, 18], which measures the independence of each IMF from the others. Low values of IO can be obtained if each extracted function is *monocomponent:* the meaning and the importance of this property will be better understood in the HT calculation that represents the following step of the process (see section 3). On the contrary, if each IMF contains more components, the IO value increases: this fact is known as *mode mixing* problem.

3. Hilbert transform algorithm

The EMD, with its sifting process, is a data-based decomposition method for the evaluation of the main components of the original signal. From a theoretical point of view, each one of these components is a monocomponent function; this implies the presence of only one component in the frequency domain. Anyhow, the achievement of only monocomponent functions is very difficult during the decomposition of experimental signals. For this reason, considering also the loose limitations related to the definition of monocomponent function, the idea of monocomponent function can be translated in terms of *narrow band* function. The extension of the validity of the characteristics of monocomponent functions to narrow band ones (i.e. the extension of the validity of the monocomponent function definition to a wide range of functions) is extremely important for the evaluation of the instantaneous frequency and for the HT more in general.

In Fourier analysis, the frequency is defined as the frequency assumed by a constant amplitude sine or cosine function fitting the original signal. As already stated, this definition is enforceable only for stationary and periodic signals. For non-stationary signals, in which frequency value changes at any moment, the definition of the *instantaneous frequency* is more appropriate. The instantaneous frequency is the frequency of a sine or a cosine function that locally fits the signal [17]. It is worth to note that, according to this definition, at least one complete oscillation of the trigonometric function is required for the evaluation of the instantaneous frequency by means of HT.

The Hilbert Transform $y(t)$ of a signal $x(t)$ is defined as [17]:

$$y(t) = \frac{1}{\pi} \int_{-\infty}^{+\infty} \frac{x(\tau)}{t-\tau} d\tau \tag{4}$$

Functions $x(t)$ and $y(t)$ are the conjugate pair that compose the analytical signal $z(t)$:

$$z(t) = x(t) + \mathrm{i}\, y(t) = a(t) \mathrm{e}^{\mathrm{i}\vartheta(t)} \tag{5}$$

Considering the last expression of the analytical signal in eq. (5), $a(t)$ can be regarded as the signal envelope and $\vartheta(t)$ the instantaneous phase. The instantaneous frequency $f(t)$ is then obtained from the last one by differentiation:

$$f(t) = \frac{1}{2\pi} \frac{\mathrm{d}\vartheta(t)}{\mathrm{d}t} \tag{6}$$

The calculation of the instantaneous frequency makes sense only for monocomponent or nearly monocomponent (i.e. narrow band) functions.

At this point, the complementarity and the effectiveness of the EMD decomposition and of the HT are evident: the former one allows obtaining functions particularly suitable for the evaluation of the instantaneous frequency by means of the subsequent Hilbert transform.

The instantaneous frequency can be calculated for each IMF extracted by the EMD algorithm. Since $f(t)$ is time-depending, the evaluation of the instantaneous frequency, for all or some of the IMF obtained, involves a 3D time-frequency distribution. For each value of time and each IMF, an instantaneous frequency can be calculated.

The 3D time-frequency distribution is known as Hilbert-Huang spectrum $H(f,t)$, where obviously f is the *instantaneous* and not the *Fourier* frequency. The instantaneous energy $IE(t)$ can be extracted from the Hilbert-Huang spectrum (HHS), by integration over the instantaneous frequency:

$$IE(t) = \int_0^f H^2(f,t)\,df \tag{7}$$

The instantaneous energy is a measure of the variation of energy over the complete signal length. Because HHS depends on the considered IMFs, also the trends and the values assumed by IE are influenced by the selected IMF.

3.1. Merit index

The choice of the IMFs to be analyzed is usually realized by means of visual or experience criteria by the user. In this way the process is not automatic and the interaction with the user is required; to make the technique faster and automatic a *merit index* (MI) has been introduced in this paper by the authors. The implemented index is, as a matter of fact, a linear combination of two indexes: the first is a measure of the periodicity degree of the IMF, while the second one is represented by its absolute skewness value.

$$MI(IMF) = P - k \cdot \left|\text{skewness}(IMF)\right|$$

$$\text{where: } P = \frac{1}{\text{std}\left[\dfrac{\max_{i+1}(IMF) - \max_i(IMF)}{\textit{period length}}\right]} \tag{8}$$

where k is a parameter specific for the considered mechanical system; for the experimental cases presented here $k=1$. To calculate *P*, a generic IMF shown in figure 1 is considered and its maximum values ($\max_i(IMF)$) exceeding a default threshold[1] (green line in figure 1) are detected; the difference between the abscissas of two consecutive maxima (green points in figure 1) are then evaluated in terms of number of points.

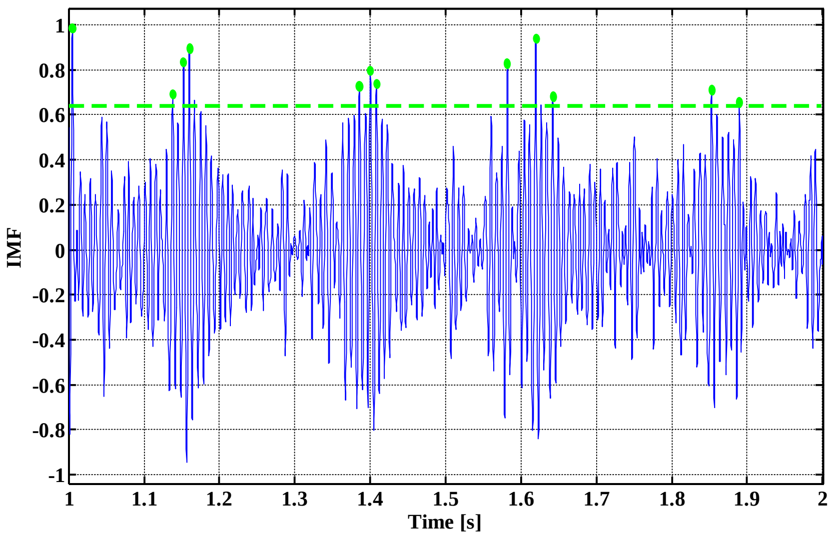

Figure 1: periodicity index calculation.

The differences, normalized with respect to the rotating period length (considering the sampling frequency), compose a set of data. The reciprocal of the standard deviation of the resulting data set represents the periodicity index *P*. If an IMF is periodical, the value assumed by the ratio in square brackets of eq. (8), for each couple of

[1] ***Note for the editor***: actually a criterion exists to find a suitable threshold for a given IMF with certain maximum amplitudes and its relationship with *k*, but the authors were allowed to publish the paper, but not to publish these details by who sponsored this research.

maxima, is about one and the resulting standard deviation is close to zero. Thanks to the standard deviation reciprocal, high values for the *P* index are obtained for periodical functions. Since no information about function symmetry is taken into account by *P* index, skewness of IMF is calculated in order to check the distribution of the function about the zero value. Since low absolute skewness values can be obtained for symmetric functions, then the merit index expressed in eq. (8) assumes high and positive values for periodical and symmetrical IMFs.
The IMF selection is very easy with the merit index: one IMF is transformed with HT if its merit index assumes a positive value.
Some words must be spent about the representation of the Hilbert-Huang spectrum: the procedure used for the instantaneous frequency evaluation gives a comparative distribution. Since the amplitude of each point in the time-instantaneous frequency plane can change depending on the length and the number of the considered IMF, the definition of a threshold value is impossible and the most important components will be those with highest amplitude. Moreover, also the diagnostics stage will be realized in a comparative way: the fault detection will be possible if its characteristic components (i.e. the signatures) dominate the spectrum.

4. Experimental test-rig

The layout of the gearbox test-rig installed in Piacenza Campus of Politecnico di Milano is shown in figure 2. The first component is an AC motor of 3.5 kW supplying power to the system and controlled by means of a control inverter. The motion is transmitted to the user unit by a spiral bevel gearbox of Gleason type with a speed ratio of 1:2 and a contact ratio between 2 and 3. The driven shaft is connected, by means of a rigid coupling, to the user unit: this is another AC motor of 2.75 kW, which provides the resistant torque. Thanks to a control software realized on purpose with LabView®, it is possible to control continuously the motor rotating speed and the user resistant torque. It is worth to note that the control software allows imposing both speed and torque variation with ramps during time in addition to constant values. This possibility assumes a great importance for benchmarking the considered technique: as stated in the introduction and as explained in the previous sections, the EMD and the following HT can be applied to the non-stationary signals.
A fault has been introduced in gearbox: one tooth of the driven wheel has been artificially removed. Since the spiral bevel gearbox is characterized by a smooth behaviour due to the high contact ratio, defects could be hidden during the operation and their detection allows evaluating the effectiveness of EMD and HT algorithms.
Different working conditions have been considered: the experimental tests have been carried out when the driving speed is in the range of 0÷2500 rpm and user resistant torque is included between 0 Nm and 10 Nm. Both constant values and ramps for the working parameters are considered.
Six channels have been acquired during each experimental test: in addition to the speed and torque signals of motor and user, vertical and horizontal vibrations have been measured by means of two industrial piezoelectric accelerometers installed on the gearbox case. The signal processing method has been tested on the vibration signals, since inverter signals have been acquired mainly for control purposes.

Figure 2: test-rig layout and driven shaft with fault.

5. Experimental results

The first example of signals acquired by means of the vertical accelerometer for the undamaged and the damaged gearbox are reported respectively in figure 3 left and right. The constant driving rotating speed is 1000 rpm and the resistant torque is set to 2.5 Nm. Only an arbitrary portion of the complete acquired signal, lasting 0.45 s, is analyzed.

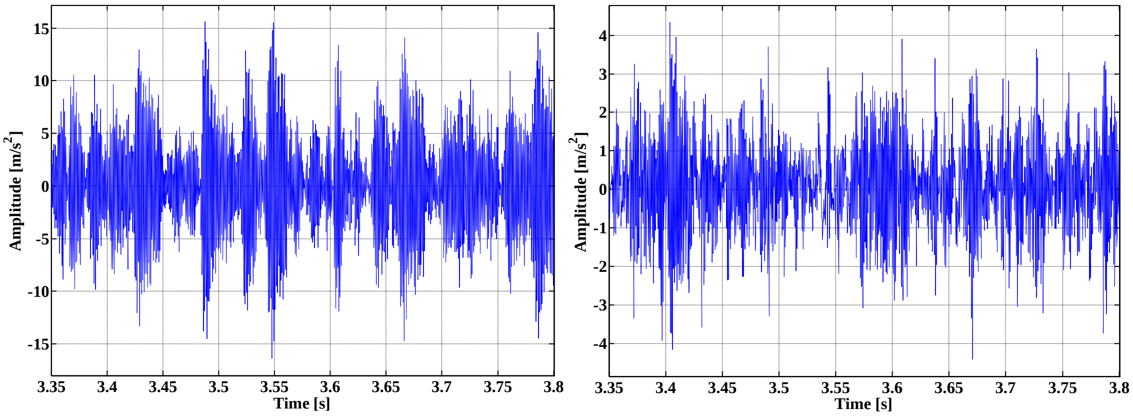

Figure 3: vertical vibrations for undamaged (left) and damaged gearbox (right).

By comparing the two time histories, it is easy to note that the highest and sudden variations of vibrations occur during the undamaged gearbox functioning. This fact can be explained by the different alignment conditions during the tests. The simple comparison of the two signals is misleading for the evaluation of the gearbox state. To discriminate the two conditions, the EMD is applied to both of the original signals: the firsts 8 IMFs extracted are reported for the undamaged gearbox and the damaged one respectively in figure 4 and figure 5.

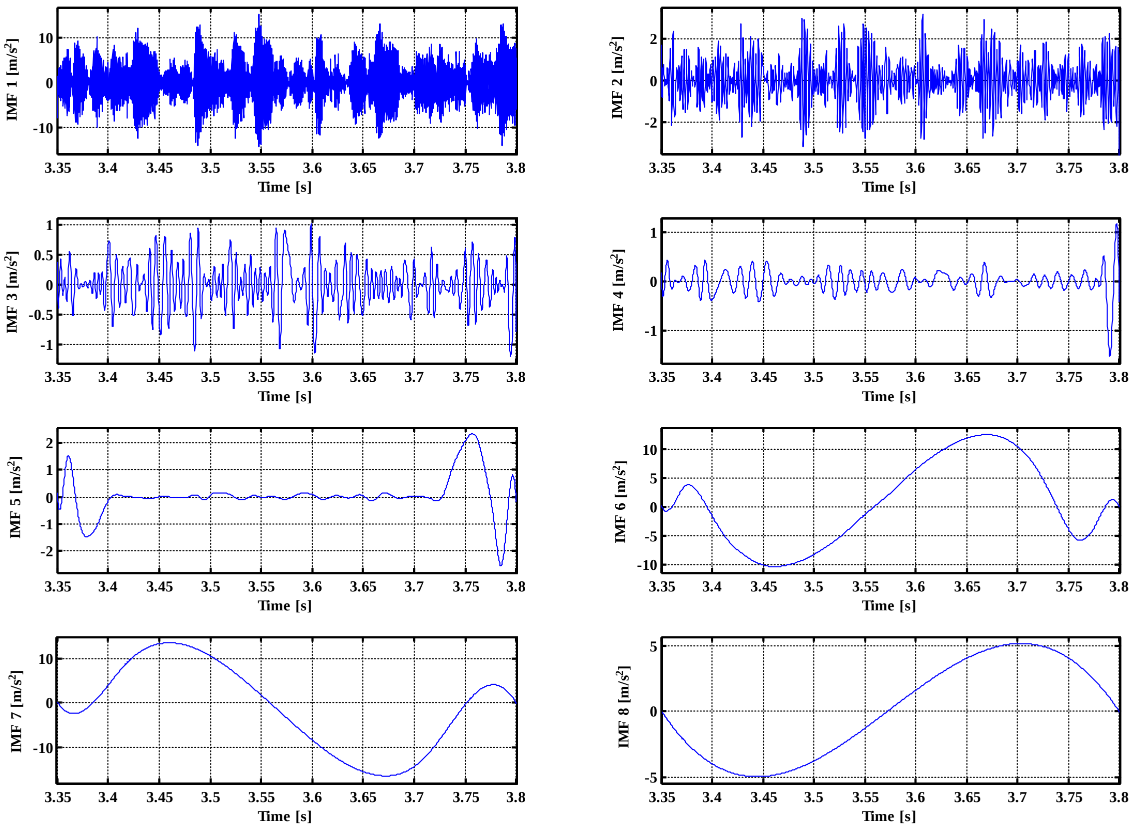

Figure 4: IMFs for the vertical vibrations signal acquired at 1000 rpm and 2.5 Nm for the undamaged gearbox.

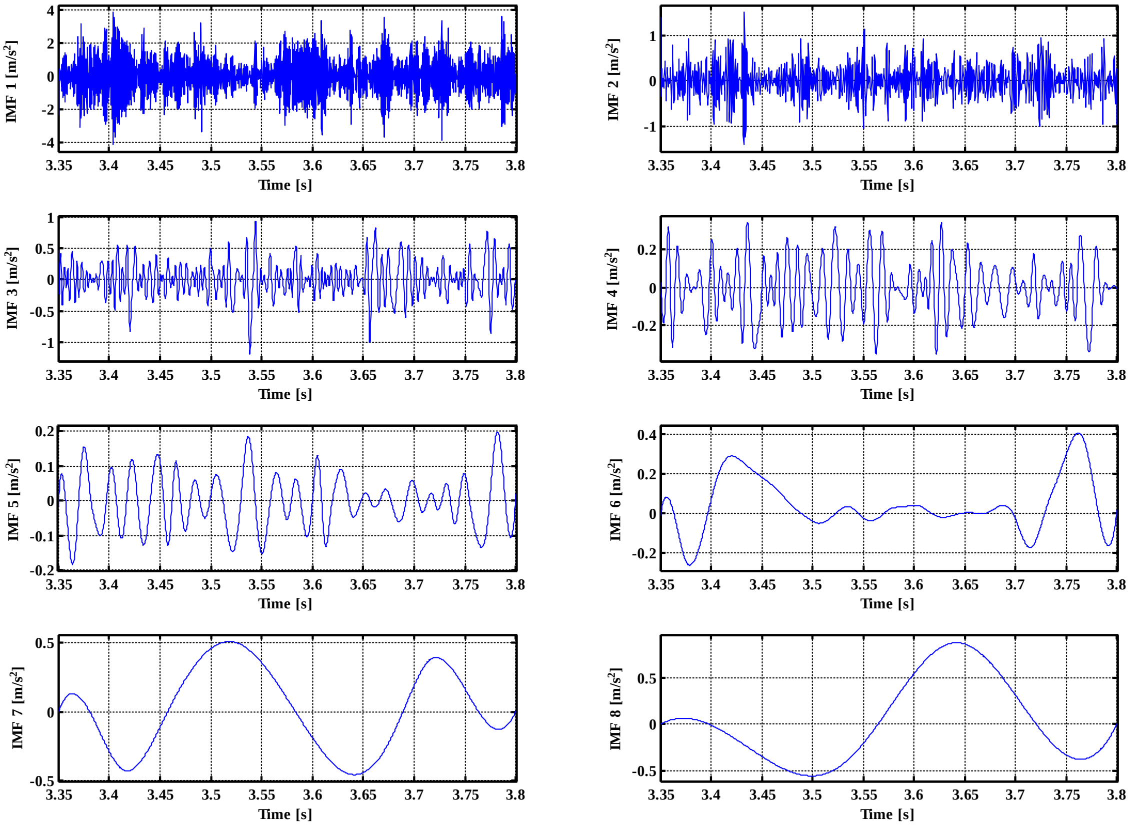

Figure 5: IMFs for the vertical vibrations signal acquired at 1000 rpm and 2.5 Nm for the damaged gearbox.

By examining the functions resulting from the decomposition, it appears that, independently from the gearbox condition, the firsts IMFs describe high frequency phenomena while the last ones are related to the low frequency components of the signals that could have not physical meaning and could be due to the stop criteria set in the sifting process. Considering that the fault signature is related to the rotation frequency, very low frequency components should not be of interest. In any case the selection of the IMF on the basis of the merit index allows these spurious IMF to be always and automatically discarded from the set used for the HT.

The one-to-one comparison between IMFs of the same order highlights differences in both shape and amplitude depending on the health condition. However the fault detection is still quite difficult at this stage: hidden variations that could be related to the fault (the removal of a tooth involves impacts during rotation, i.e. it excites transients) can be traced in the decompositions even if in different IMFs. Obviously, in accord with the previous remarks, not all the IMFs are considered for HT.

The merit index for each IMF has been evaluated using eq. (8): the values assumed by the parameter for the undamaged and damaged gearbox are reported respectively in table 1 and table 2. Positive values are obtained by IMF 1 and 3 for the undamaged gearbox, while higher values of MI are reached by the IMF 3 and 4 for the damaged one. These are the IMFs chosen by the algorithm and subjected to HT.

Table 1: merit index evaluation for the vertical vibrations IMFs (undamaged gearbox).

IMF	periodicity index	absolute skewness	merit index
1	2.037	0.003	2.034
2	0.000	0.042	-0.042
3	0.806	0.156	0.650
4	0.000	1.067	-1.067
5	0.000	0.405	-0.405
6	0.000	0.163	-0.163
7	0.000	0.141	-0.141
8	0.000	0.000	0.000

Table 2: merit index evaluation for the vertical vibrations IMFs (damaged gearbox).

IMF	periodicity index	absolute skewness	merit index
1	1.986	0.015	1.971
2	0.722	0.077	0.645
3	4.053	0.122	3.931
4	2.111	0.002	2.109
5	1.039	0.127	0.912
6	0.000	0.584	-0.584
7	0.000	0.014	-0.014
8	0.000	0.598	-0.598

Hilbert-Huang spectra for the undamaged and damaged gearbox are shown in figure 6, where the 3D representation is flatten in a plane and dark colours indicate high values of the spectrum. HHS highlights a homogeneous distribution along the time axis for the undamaged gearbox (figure 6 left); in other words, no regions with higher amplitudes than others are evident. The presence of frequency bands depends instead on the IMFs analyzed; it is worth to note again that the values of the instantaneous frequency are not related to any mechanical frequency. The meaning of the instantaneous frequency is then different from the traditional definition. HHS of the damaged gearbox (figure 6 right) is quite different from the previous one: the time-instantaneous frequency plot is dominated by some regions located at low values of the instantaneous frequency and spaced in time by 0.12 s, i.e. the period of the fault at the user rotating speed of 500 rpm.

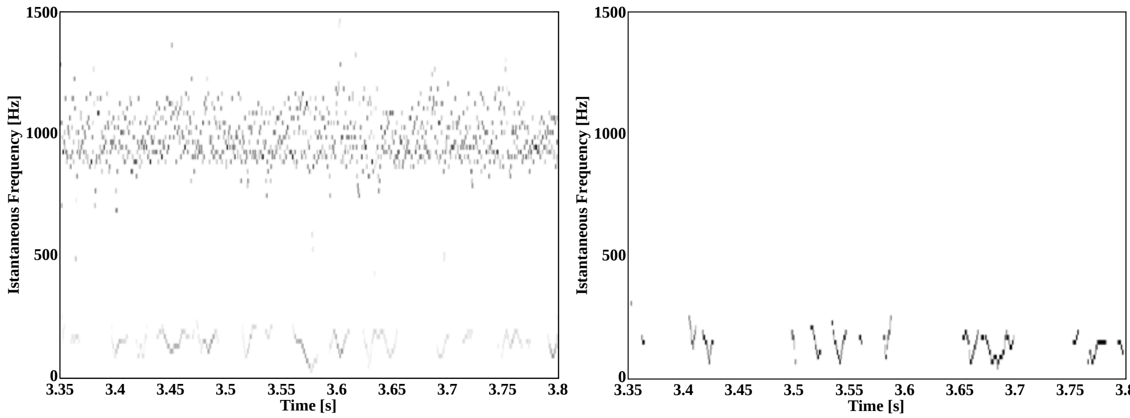

Figure 6: HHS for the undamaged (left) and damaged (right) gearbox.

The fault detection and location is, if possible, easier by means of IE evaluation: the trends for the undamaged and damaged gearbox are shown in figure 7.

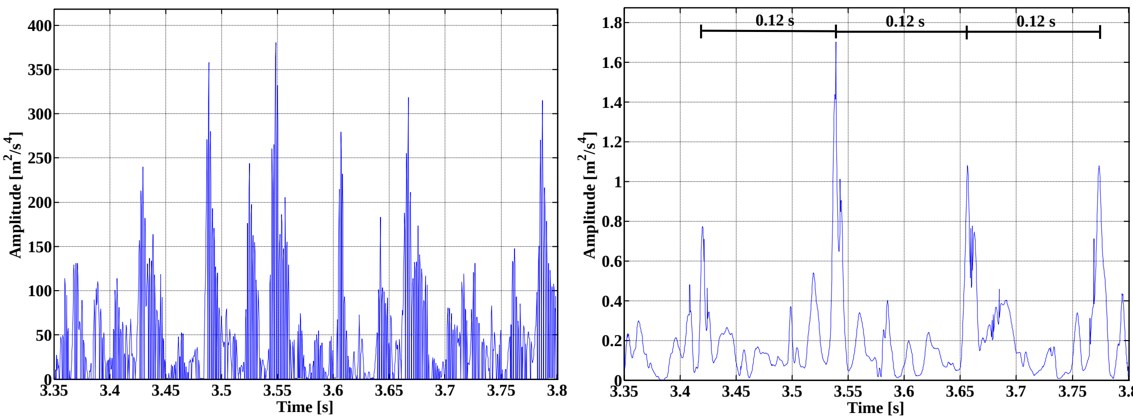

Figure 7: IE for the undamaged (left) and damaged (right) gearbox.

In order to interpret correctly figure 7, it is important to bear in mind that the higher vibrations of the undamaged gearbox were caused by bad alignment in this test. For the damaged gearbox, the instantaneous energy is strictly connected to energy introduction in the system by the fault, which is predominant with respect to that introduced by other meshing teeth.
This causes a sort of "regularization" of the peaks, i.e. the relative increasing of the components due to the fault with respect to the components due to the rotation and with the period of 0.12 s related to fault presence. This result, highlighted by IE, is the same obtained by the comparison of the HHS of figure 6.
Moreover, the IE is calculated on the basis of the selected IMF, which are influenced by the original signal RMS value. Thus the RMS or the mean value of the IE could be higher for the undamaged than for the damaged gearbox, but what the most important thing is that the peaks unevenly spaced in the time of the undamaged gearbox tends to become periodical for the damaged one.
Also the vibrations acquired by the horizontal accelerometer has been analyzed in the same working conditions. The signal interval taken into consideration is the same of the previous case, in order to compare both the IMFs extraction process and the results of HT with those obtained for the vertical accelerometer. As already seen, the diagnosis based on signals only can be misleading: also in this case the vibration amplitude for the undamaged transmission, which exceeds 3 m/s^2 (figure 8 left), is greater than that of the damaged one, whose maximum is about 2 m/s^2 (figure 8 right).

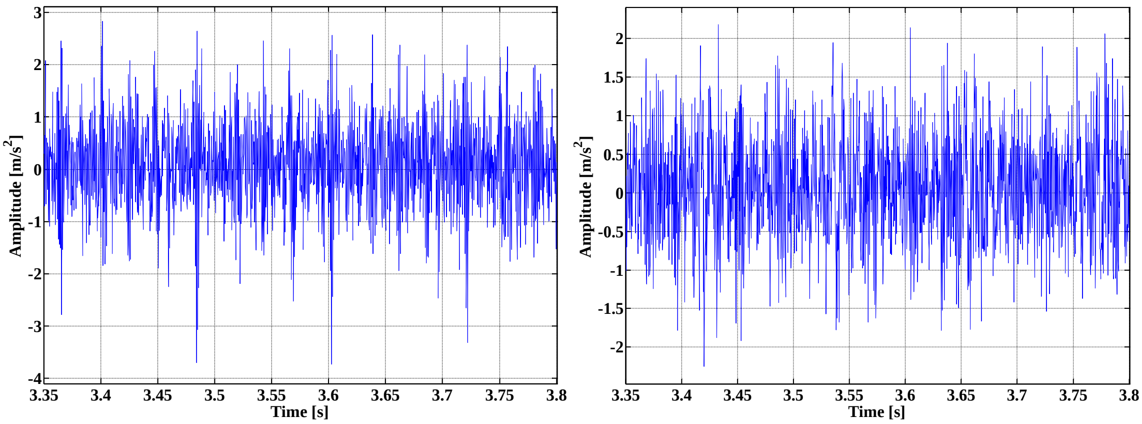

Figure 8: lateral vibrations for undamaged (left) and damaged gearbox (right).

The IMFs extracted from the two signals by means of EMD are shown in figure 9 and figure 10. Contrary to the previous case, the one-to-one comparison between the IMFs of the same order suggests the presence of the fault, while high-order IMFs could not have physical meaning.

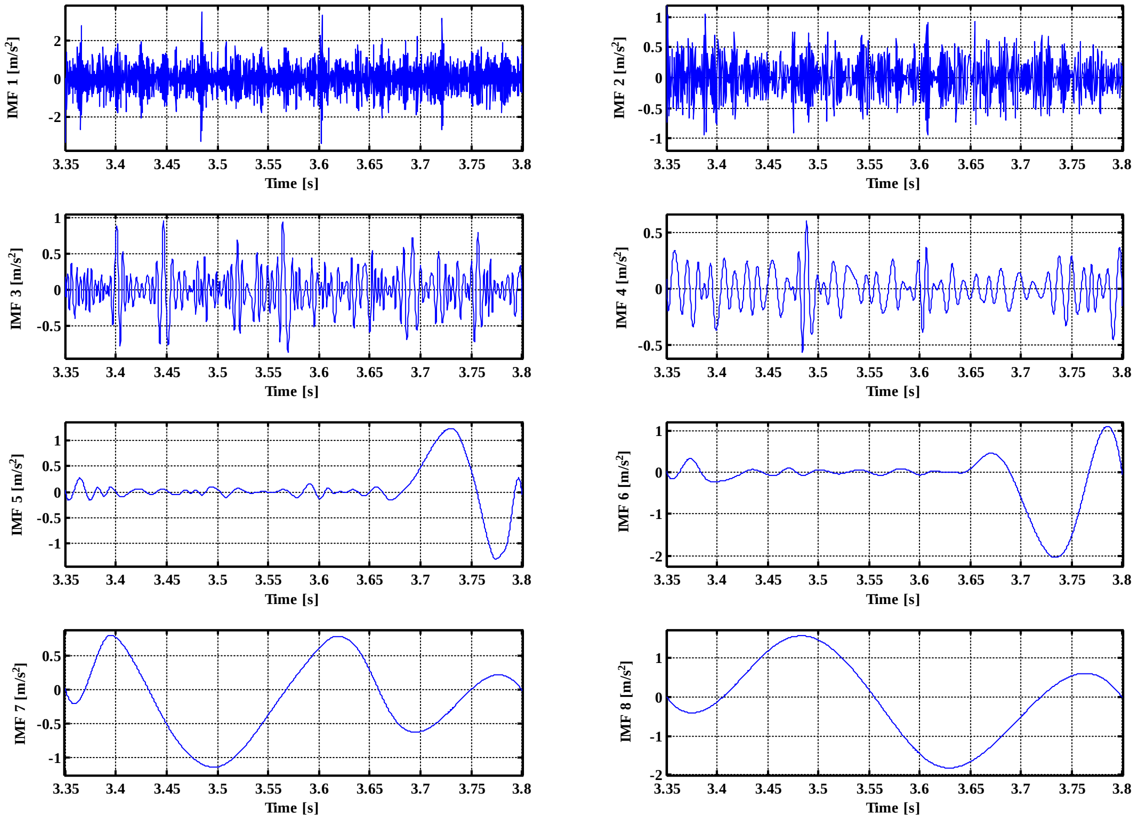

Figure 9: IMFs for the lateral vibrations signal acquired at 1000 rpm and 2.5 Nm for the undamaged gearbox.

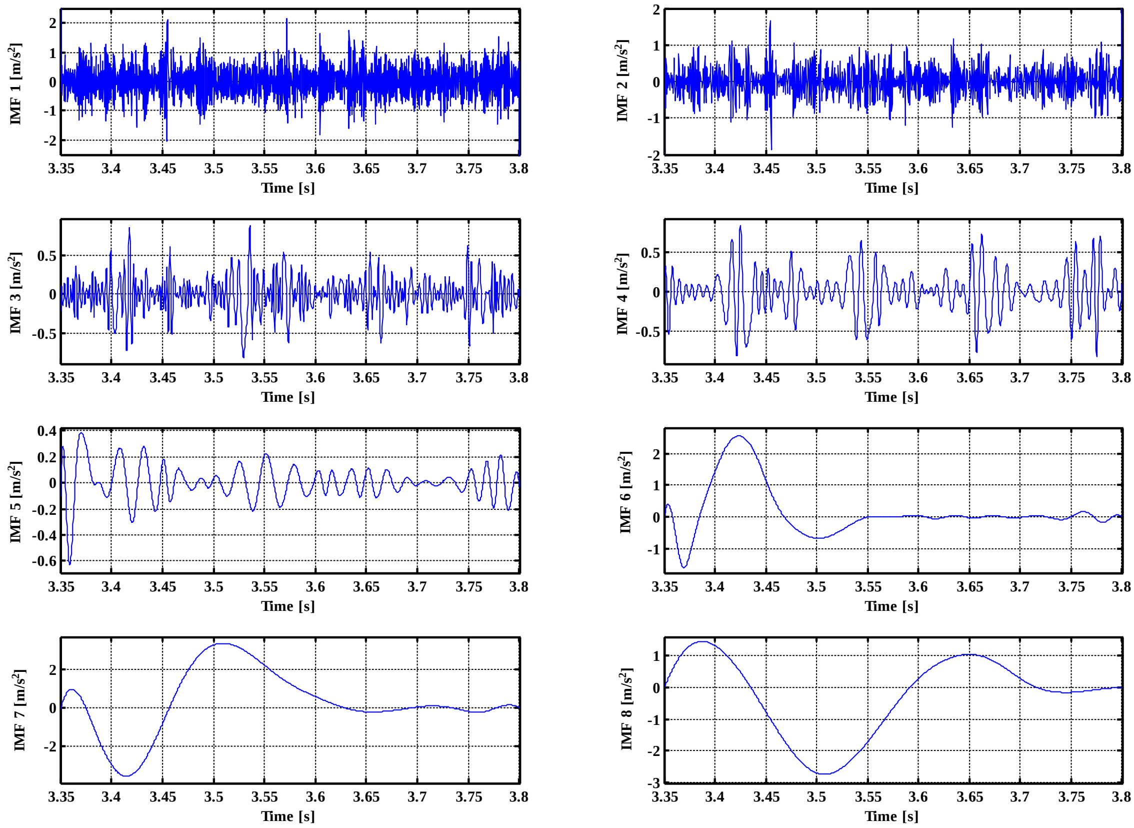

Figure 10: IMFs for the lateral vibrations signal acquired at 1000 rpm and 2.5 Nm for the damaged gearbox.

The periodical transients (amplitude variations) appearing in the third and the fourth IMFs of figure 10 are revealing of the abnormal functioning of the system. Similarly to the previous signals, MI has been evaluated and the results are reported in table 3 and table 4 respectively for the undamaged gearbox and the damaged one. The IMFs with positive values of MI are those selected by the algorithm for HT (i.e. IMF 1, 2 and 3 are chosen for the undamaged gearbox and IMF 3 and 4 are considered for that without one tooth). Note that high-order IMFs are again automatically discarded.

Table 3: merit index evaluation for the lateral vibrations IMFs (undamaged gearbox).

IMF	periodicity index	absolute skewness	merit index
1	2.688	0.027	2.661
2	1.436	0.369	1.067
3	1.461	0.058	1.402
4	0.000	0.072	-0.072
5	0.000	0.045	-0.045
6	0.000	1.586	-1.586
7	0.000	0.119	-0.119
8	0.000	0.195	-0.195

Table 4: merit index evaluation for the lateral vibrations IMFs (damaged gearbox).

IMF	periodicity index	absolute skewness	merit index
1	0.000	0.208	-0.208
2	0.000	0.042	-0.042
3	2.615	0.097	2.518
4	12.522	0.046	12.477
5	0.000	0.508	-0.508
6	0.000	1.527	-1.527
7	0.000	0.232	-0.232
8	0.000	0.717	-0.717

The Hilbert-Huang spectra obtained for the two conditions are reported in figure 11. They are similar to those obtained for the vertical vibration signals: the distribution is quite homogeneous in the time-frequency plane (i.e. the energy is equally distributed) for the undamaged gearbox (figure 11 left), while regions with high amplitude are located at low values of the instantaneous frequency and spaced in time with the same period of the fault signature for the damaged gearbox (figure 11 right).

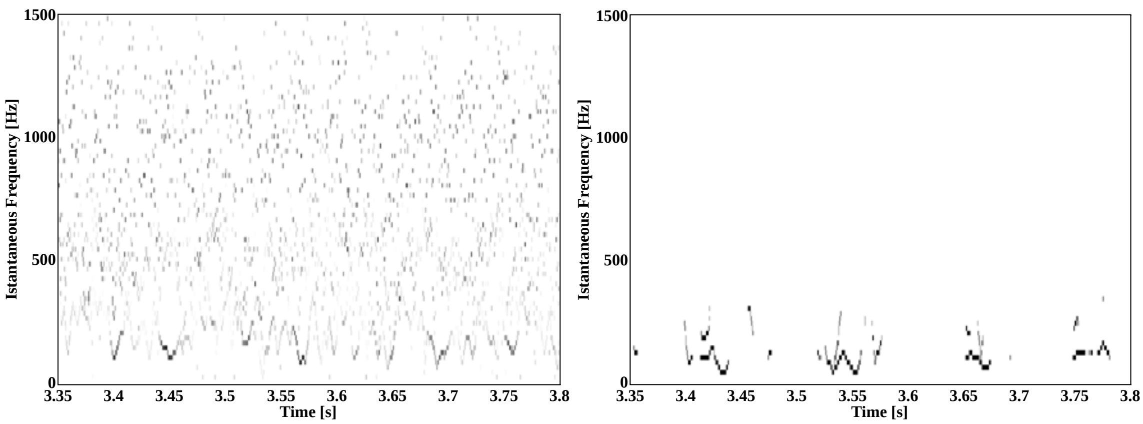

Figure 11: HHS for the undamaged (left) and damaged (right) gearbox.

The IE trends derived from the two Hilbert-Huang spectra are shown in figure 12; while the first plot is characterized by several peaks unevenly spaced in time, the second plot presents periodical peaks spaced by 0.12 s, related to the tooth absence, which clearly indicates the fault. As a matter of fact, even in presence of high contact ratio, the tooth absence causes collisions involving the instantaneous increase of energy.

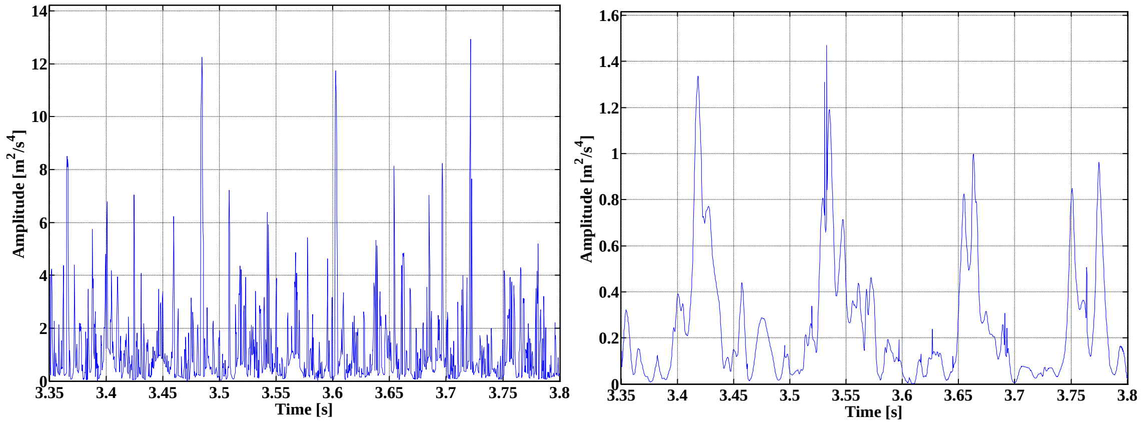

Figure 12: IE for the undamaged (left) and damaged (right) gearbox.

With the aim to confirm the very good results provided by the proposed approach in correspondence of light duty conditions, heavier working conditions are now considered. The horizontal vibration signals acquired for motor rotating speed of 2000 rpm and resistant torque of 7.5 Nm for undamaged and damaged gearbox are shown in figure 13. Also in this case, complete time histories are not examined: only the time interval from the 3.6 s up to 3.85 s is considered for both gearbox vibrations. The comparison between the two signals suggests the same remarks already discussed for the previous operating conditions: contrarily to the common sense, the vibration amplitude is greater for the undamaged transmission than for the damaged one.

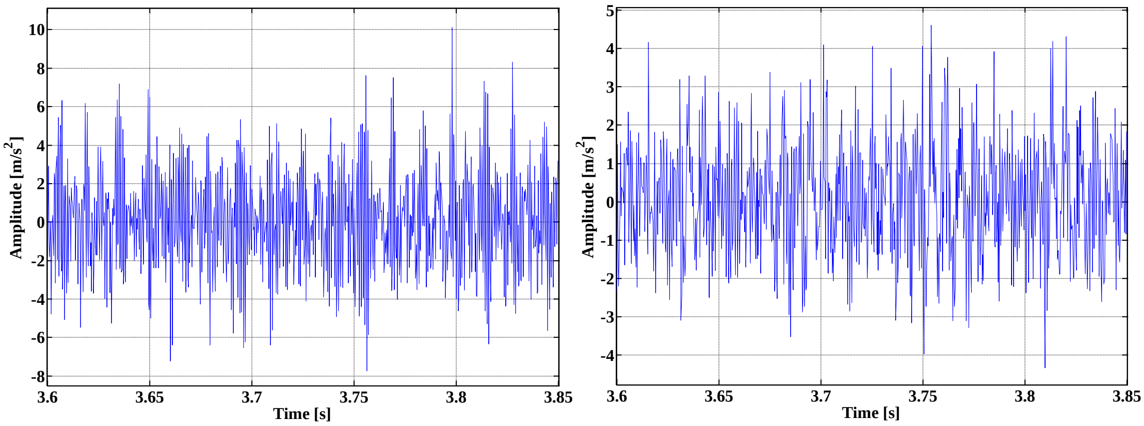

Figure 13: lateral vibrations for undamaged (left) and damaged gearbox (right).

The results of EMD are reported in figure 14 and figure 15. The IMFs are quite similar for the two gearboxes and at sight the detection of the fault should not be allowed. Since the only MI positive value is obtained for the first IMF of figure 14 for the undamaged gearbox (see table 5), HT is carried out only over that function. The resulting HHS is shown in figure 16 left; no concentration of energy is highlighted and this indicates the correct functioning of the gearbox.

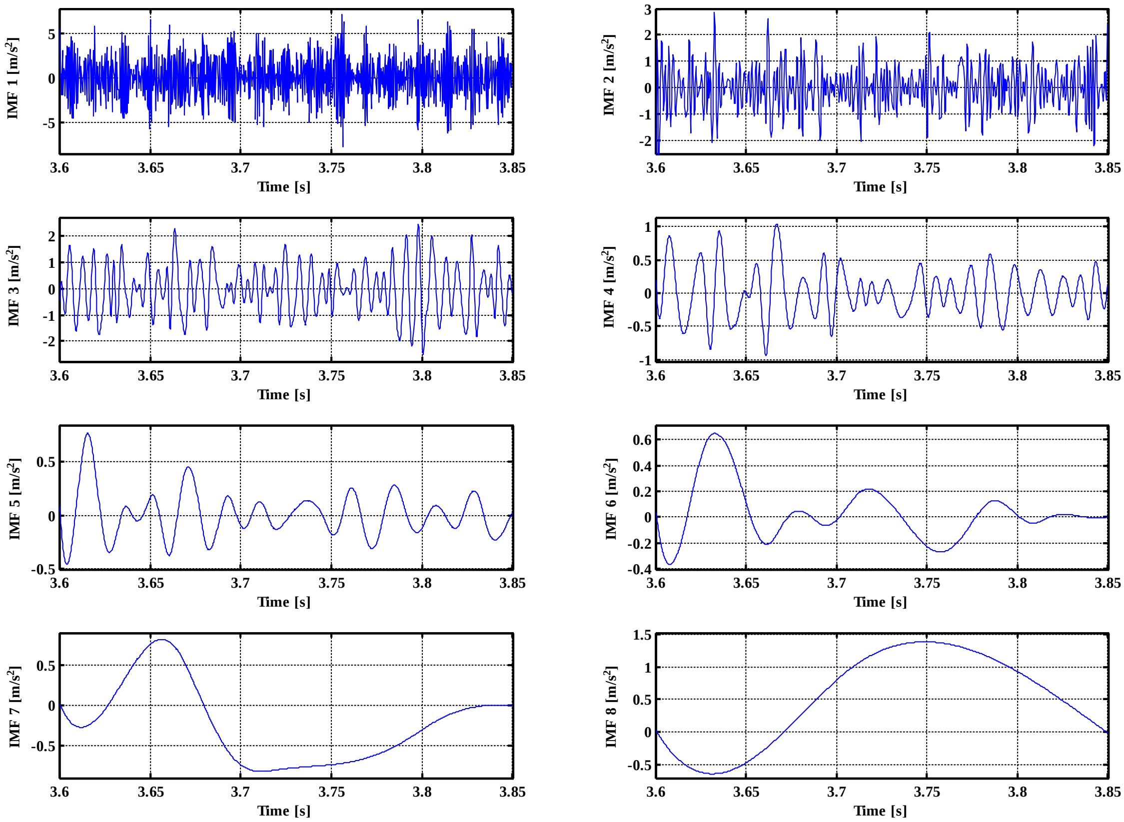

Figure 14: IMFs for the lateral vibrations signal acquired at 2000 rpm and 7.5 Nm for the undamaged gearbox.

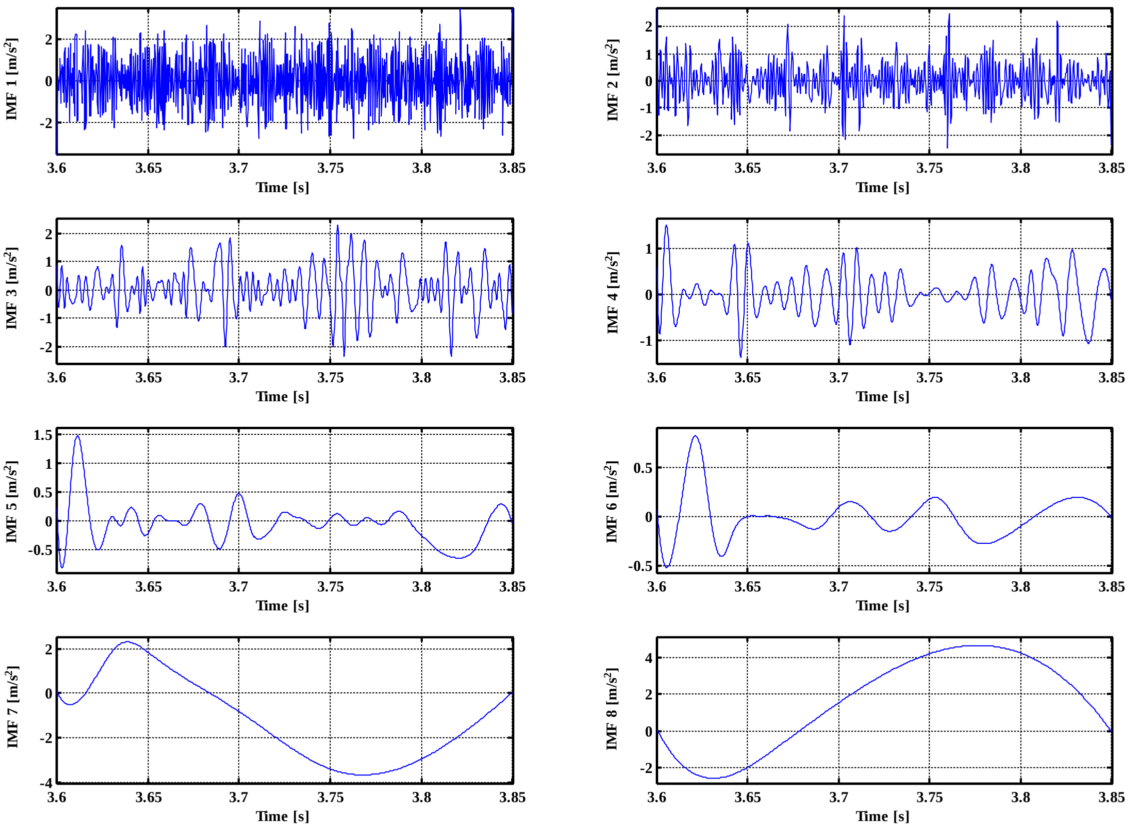

Figure 15: IMFs for the lateral vibrations signal acquired at 2000 rpm and 7.5 Nm for the damaged gearbox.

For the damaged gearbox, the positive values of the MI are those corresponding to IMFs 2, 3 and 4 (see table 6).

Table 5: merit index evaluation for the lateral vibrations IMFs (undamaged gearbox).

IMF	periodicity index	absolute skewness	merit index
1	2.102	0.044	2.057
2	0.000	0.871	-0.871
3	0.000	0.054	-0.054
4	0.000	0.268	-0.268
5	0.000	0.761	-0.761
6	0.000	1.044	-1.044
7	0.000	0.632	-0.632
8	0.000	0.294	-0.294

Table 6: merit index evaluation for the lateral vibrations IMFs (damaged gearbox).

IMF	periodicity index	absolute skewness	merit index
1	0.000	0.253	-0.253
2	1.177	0.128	1.048
3	1.856	0.085	1.771
4	1.279	0.132	1.146
5	0.000	1.150	-1.150
6	0.000	0.995	-0.995
7	0.000	0.255	-0.255
8	0.000	0.317	-0.317

The corresponding HHS (figure 16 right) highlights four localized regions in which the amplitude is greater than in the remaining plane. The difference between the two Hilbert-Huang spectra can be easily traced also considering the IE trends: periodical peaks with higher amplitude are highlighted for the damaged gearbox (figure 17 right).

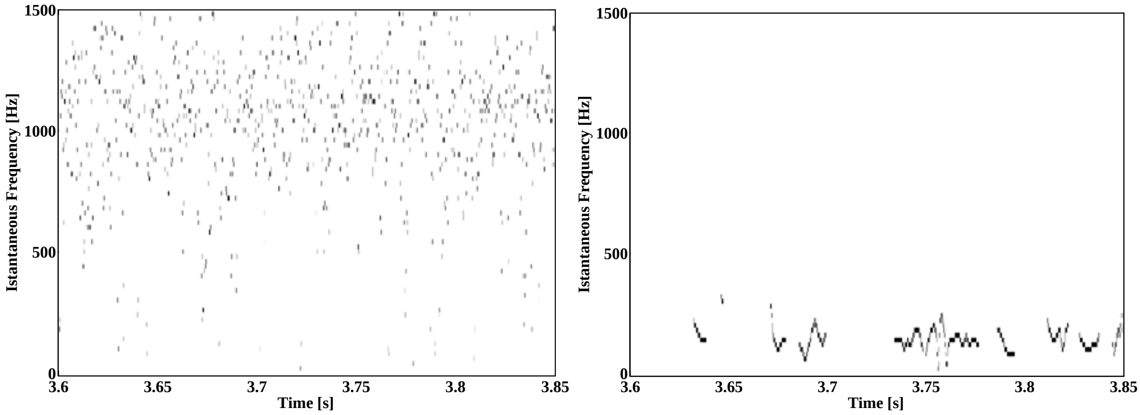

Figure 16: HHS for the undamaged (left) and damaged (right) gearbox.

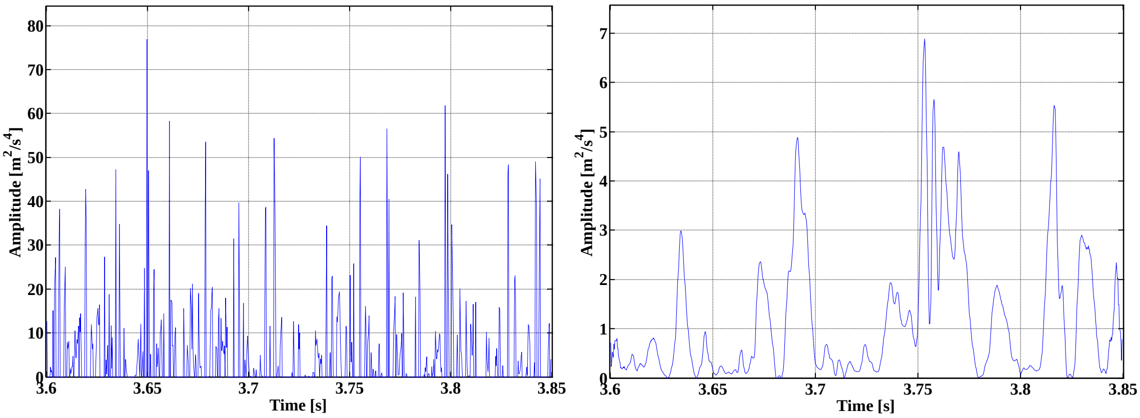

Figure 17: IE for the undamaged (left) and damaged (right) gearbox.

Since no hypothesis about the stationarity and the periodicity of the signal must respected for EMD and HT application, the considered approach is tested on data collected during a speed transient for the damaged gearbox. Motor rotating speed has the variation of 100 rpm/s and the resistant torque is 5 Nm. A window of 1 s length of the motor speed signal is shown in figure 18 (left), while the corresponding vertical vibration signal is reported in figure 18 (right).

The amplitude of the signal does not change considerably during the speed transient and there is no evidence of fault.

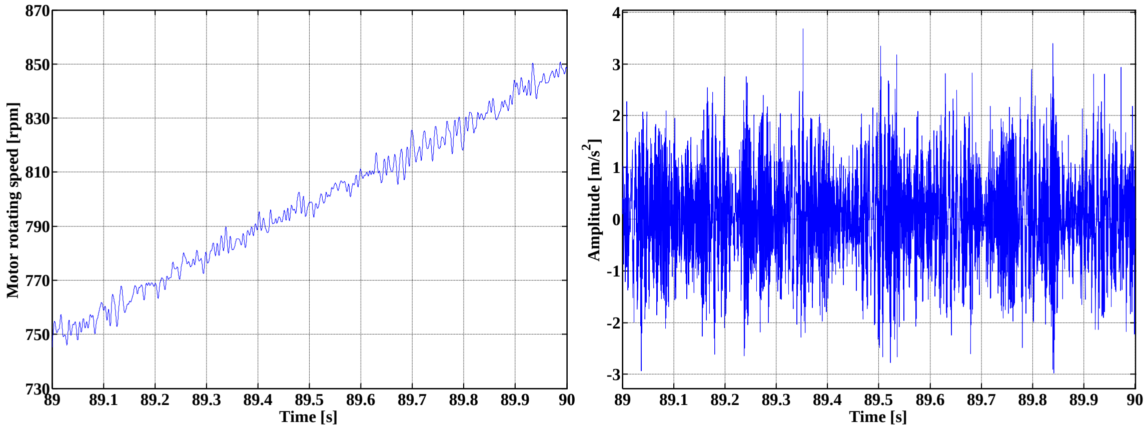

Figure 18: driving rotating speed transient (left) and lateral vibrations signal (right).

EMD is applied and the extracted IMFs are shown in figure 19. Fault signature already appears at this stage: the third IMF is affected by periodical variation of amplitude.

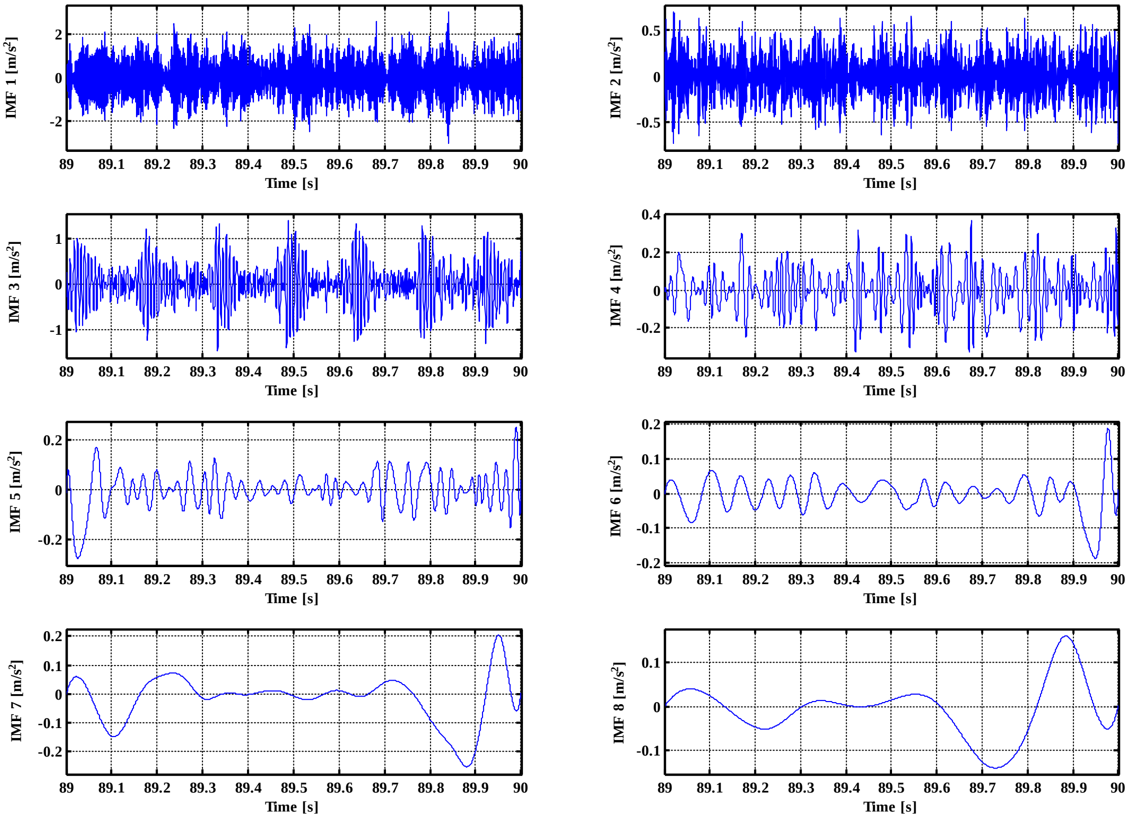

Figure 19: IMFs of the vertical vibrations signal for the damaged gearbox.

In this case, highest MI values are obtained for IMFs from 1 to 4, see table 7. Obviously a high value was already expected for IMF 3. HHS obtained after HT is shown in figure 20 left. The tooth absence is indicated by the regions with high amplitude at low values of the instantaneous frequency, seven regions are highlighted. Moreover, the distance between the regions decreases with the time: this is due to the system rotating speed increasing during the considered time interval.

Table 7: merit index evaluation for the vertical vibrations IMFs (damaged gearbox).

IMF	periodicity index	absolute skewness	merit index
1	0.558	0.003	0.556
2	1.837	0.029	1.808
3	1.562	0.007	1.554
4	0.592	0.018	0.574
5	0.000	0.628	-0.628
6	0.000	0.556	-0.556
7	0.000	0.783	-0.783
8	0.000	0.123	-0.123

The instantaneous energy has been estimated also in this case; its trend during the considered time interval is shown in figure 20 right. The presence of the fault is evident if the peaks exceeding the 1.5 m^2/s^4 value are considered. Their spacing changes from 0.16 s to 0.141 s corresponding to the user rotating speed of 375 and 425 rpm respectively.

Fault detection by means of IE seems more evident for the last case considered, with variable rotating speed, than for the previous ones.

Being the EMD a data-based decomposition and HT a method for the instantaneous frequency evaluation, it is possible that the already good results obtained for practically stationary and periodical signals (steady state

condition) can be still improved for transient signals, intrinsically characterized by continuous variations of its values and conditions.
This remark is very important, above all from an operational point of view: the robustness and the diagnostics effectiveness of the technique, independently from the gearbox working conditions, make it very useful for on-line diagnostics of mechanical systems.

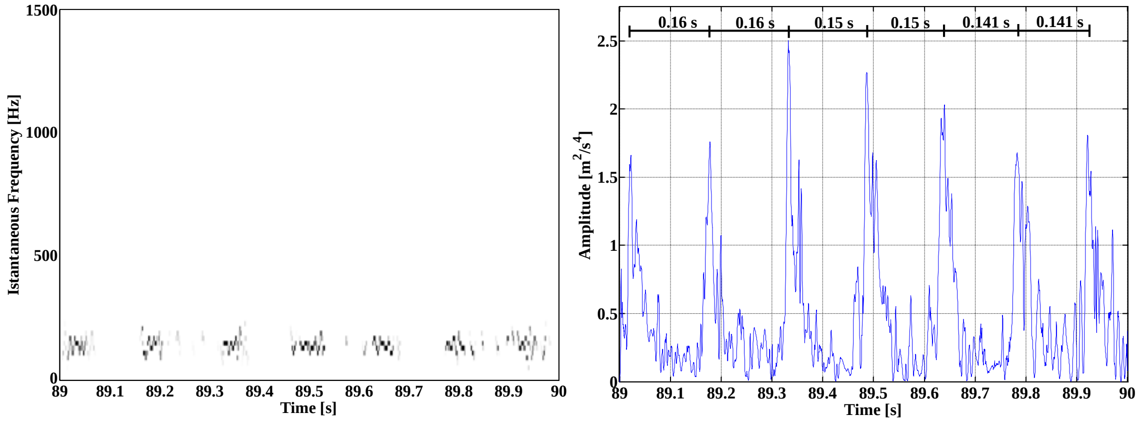

Figure 20: HHS (left) and IE (right) for the damaged gearbox.

6. Conclusions

The aim of the paper is the improvement of EMD and HT by means of the introduction of a suitable merit index that allows the automatic selection of the IMF. This overcomes a major limit of the traditional EMD-HT technique and allows the development of on-line tools. Indeed, not all the IMFs obtained by the decomposition should be considered in HT; until now the choice was realized case by case by the user with trial or experience criteria.
The automatic selection proposed allows successful diagnosis of a damaged gearbox installed in a test-rig, in different operating conditions, including also transient conditions. In this way, the powerful characteristics of EMD-HT are fully exploited. It is also worth to note, that the gearbox tested was a spiral bevel one, which is characterized by rugged design and very smooth operation, with contact ratio between 2 and 3. The high contact ratio causes that the deliberated breaking of a tooth of the driven gear has no effect on the motion transmission, as documented in the paper, since considering direct vibration signals only, the damaged gearbox looks like “quieter” than the damaged one. This notwithstanding, the automatic procedure proposed to select the IMF allows identifying correctly the damaged gearbox.

References

[1] P.D. McFadden, Interpolation techniques for time domain averaging of gear vibration, Mechanical System and Signal Processing 3(1) (1989) 87-97.

[2] P.D. McFadden, Examination of a technique for the early detection of failure in gears by signal processing of the time domain average of the meshing vibration, Mechanical System and Signal Processing 1(2) (1987) 173-183.

[3] P.D. McFadden, J.D. Smith, A signal processing technique for detecting local defects in gears from the signal average of the vibration, Proceedings of the Institute of Mechanical Engineers 199(C4) (1985) 287-292.

[4] W. J. Staszewski, G. R. Tomlinson, Application of the wavelet transform to fault detection in a spur gear, Mechanical System and Signal Processing 8(3) (1994) 289-307.

[5] D. Boulahbal, M.F. Golnaraghi, F. Ismail, Amplitude and Phase Wavelet Maps for the Detection of Cracks in Geared Systems, Mechanical Systems and Signal Processing 13(3) (1999) 423-436.

[6] J. Lin, L. Qu, Feature Extraction Based on Morlet Wavelet and its Application for Mechanical Fault Diagnosis, Journal of Sound and Vibration 234(1) (2000) 135-148.

[7] Y. Ohue, A. Yoshida, M. Seki, 2004, Application of the Wavelet Transform to Health Monitoring and Evaluation of Dynamic Characteristics in Gear Sets, Proceedings of the IMechE Journal of Engineering Tribology 218(1) (2004) 1-11.

[8] C. Capdessus, M. Sidahmed, J.L. Lacoume, Cyclostationary Processes: Application in Gear Faults Early Diagnosis, Mechanical Systems and Signal Processing 14(3) (2000) 371-385.

[9] R. B. Randall, J. Antoni, S. Chobsaard, The relationship between spectral correlation and envelope analysis in the diagnostics of bearing faults and other cyclostationary machine signals, Mechanical System and Signal Processing 15(5) (2001) 945-962.

[10] R. B. Randall, Detection and diagnosis of incipient bearing failure in helicopter gearboxes, Engineering Failure Analysis 11(1) (2004) 177-190.

[11] J. Antoni, Cyclostationarity by examples, Mechanical System and Signal Processing 23(4) (2009) 987-1036.

[12] M. E. Badaoui, J. Antoni, F. Guillet, J. Danière, P. Velex, Use of the moving cepstrum integral to detect and localise tooth spalls in gears, Mechanical System and Signal Processing 15(5) (2001) 873-885.

[13] N. J. Wismer, Gearbox Analysis using Cepstrum Analysis and Comb Liftering, Application Note Brüel & Kjær 1994.

[14] W. Wang, Early Detection of Gear Tooth Cracking Using the Resonance Demodulation Technique, Mechanical Systems and Signal Processing 15(5) (2001) 887-903.

[15] R. Ricci, P. Pennacchi, Diagnostics of a spiral bevel gearbox using signals of the motor inverter, 9th International Conference on Vibrations in Rotating Machinery IMechE 2008 C663-058 1-10.

[16] G. Dalpiaz, A. Rivola, R. Rubini, Effectiveness and Sensitivity of Vibration Processing Technique for Local Fault Detection in Gears, Mechanical Systems and Signal Processing 14(3) (2000) 387-412.

[17] N. E. Huang, Z. Shen, S. R. Long, M. C. Wu, H. H. Shih, Q. Zheng, N.-C. Yen, C. C. Tung, H. H. Liu, The empirical mode decomposition and the Hilbert spectrum for nonlinear and non-stationary time series analysis, Proceedings of the Royal Society of London Series A 454 (1998) 903–995.

[18] S. J. Loutridis, Damage detection in gear systems using empirical model decomposition, Engineering Structures 26(12) (2004) 1833-1841.

[19] Y. Lei, Z. He, Y. Zi, Application of the EEMD method to rotor fault diagnosis of rotating machinery, Mechanical System and Signal Processing 23(4) (2009) 1327-1338.

[20] A. Parey, M E. Badaoui, F. Guillet, N. Tandon, Dynamic modelling of spur gear pair and application of empirical mode decomposition-based statistical analysis for early detection of localized tooth defect, Journal of Sound and Vibration 294(3) (2006) 547-561.

[21] W. Yang, P.J. Tavner, Empirical mode decomposition, an adaptive approach for interpreting shaft vibratory signals of large rotating machinery, Journal of Sound and Vibration 321(3-5) (2009) 1144-1170.

[22] B. C. Lovell, R. C. Williamson, B. Boashash, The relationship between instantaneous frequency and time-domain representations, IEEE Transaction on Signal Processing 41(3) (1993).

[23] D. Bernal, B. Gunes, An examination of instantaneous frequency as a damage detection tool, Proceedings of 14th Engineering Mechanics Conference, Austin, TX, (2000) 398-405.

[24] B. C. Schwartz, D. L. Jones, Quadratic and instantaneous frequency analysis of helicopter gearbox faults, Mechanical System and Signal Processing 14(4) (2000) 579-595.

[25] C. Junsheng, Y. Dejie, Y. Yu, Research on the intrinsic mode function (IMF) criterion in EMD method, Mechanical Systems and Signal Processing 20(4) (2006) 817-824.

[26] D. Yu, Y. Yang, J. Cheng, Application of time-frequency entropy method based on Hilbert-Huang transform to gear fault diagnosis, Measurement 40(9-10) (2007) 823-830.

[27] H. Li, X. Deng, H. Dai, Structural damage detection using the combination method of EMD and wavelet analysis, Mechanical System and Signal Processing 21(1) (2007) 298-306.

[28] F. Wu, L. Qu, Diagnosis of subharmonic faults of large rotating machinery based on EMD, Mechanical System and Signal Processing 23(2) (2009) 467-475.

[29] F.L. Litvin, Gear Geometry and Applied Theory, Prentice-Hall, Englewood Cliffs (1994) 631-635.